Title:

Efficient assembly and long-term stability of defensive microbiomes via private resources and community bistability

Running title:

Microbiomes via private resources and bistability

Authors:

Gergely Boza[1,2,*], Sarah F. Worsley[3], Douglas W. Yu[3,4,5], and István Scheuring[1,6]

Affiliations:

[1]Evolutionary Systems Research Group, MTA-ÖK-BLI Centre for Ecological Research, Hungarian Academy of Sciences, Tihany, Hungary; [2]International Institute for Applied Systems Analysis (IIASA), Laxenburg, Austria; [3]School of Biological Sciences, University of East Anglia, Norwich Research Park, Norwich, United Kingdom; [4]State Key Laboratory of Genetic Resources and Evolution, Kunming Institute of Zoology, Chinese Academy of Sciences, Kunming, Yunnan, 650223, China; [5]Center for Excellence in Animal Evolution and Genetics, Chinese Academy of Sciences, Kunming Yunnan, 650223 China; [6]MTA-ELTE Theoretical Biology and Evolutionary Ecology Research Group, Hungarian Academy of Sciences, Budapest, Hungary.

[*] Email: boza.gergely5@gmail.com; boza@iiasa.ac.at; Telephone number: +36-1-372-2500/1706; Address: Klebelsberg Kunó str. 3, H-8237 Tihany, Hungary.

The authors declare no conflict of interest.

Abstract

Understanding the mechanisms promoting the assembly and maintenance of host-beneficial microbiomes is an open problem. An increasing amount of evidence supports the idea that animal and plant hosts can use 'private resources' and the ecological phenomenon known as 'community bistability' to favour some microbial strains over others. We briefly review empirical evidence showing that hosts can: (i) protect the growth of beneficial strains in an isolated habitat, (ii) use antibiotic compounds to suppress non-beneficial, competitor strains, and (iii) provide resources (for a limited time) that only beneficial strains are able to translate into an increased rate of growth, reproduction, or antibiotic production. We then demonstrate in a spatially explicit, individual-based model that these three mechanisms act similarly by selectively promoting the initial proliferation of preferred strains, that is, by acting as a private resource. By explicitly modelling localized microbial interactions and diffusion dynamics, we further show that an intermediate level of antibiotic diffusion is the most efficient mechanism in promoting preferred strains and that that there is a wide range of conditions under which hosts can promote the assembly of a self-sustaining defensive microbiome. This, in turn, supports the idea that hosts readily evolve to promote host-beneficial defensive microbiomes.

Introduction

A growing number of studies show that microbiome composition is structured by competition [1, 2, 3, 4, 5, 6, 7], and it is hypothesized that a host could evolve to bias these processes to promote the establishment of host-beneficial microbes [6, 8, 9, 10, 11, 12, 13]. Indeed, such microbes need support because, first, it is inherently difficult to establish a colony of host-beneficial microbes in the face of competition against the huge pool of available host-neutral or host-harmful species [1, 14, 15, 16, 17], and second, these microbes often produce costly compounds that, although equipping them to be beneficial for the host, render them competitively inferior to non-beneficial, or even parasitic, microbes [18].

We distinguish three mechanisms by which a host can selectively favour beneficial strain(s), namely (1) *providing a habitable space* that the desired bacterial partner has preferential access to, (2) *production of specific compounds* by the host that selectively poison undesired bacteria, and (3) *providing a food resource* that the desired partner is better able to metabolise. We now briefly review examples of each:

1. *Providing a habitable space that the desired bacterial partner has preferential access to.* — Vertical and pseudo-vertical transmissions fall into this category [1, 19, 20, 21, 22, 23]. In strict vertical transmission, host germline cells are infected with symbionts [22, 24]. Less strict transmission ('pseudo-vertical') is achieved by keeping non-colonised host offspring in isolation after birth until the parental microbiome can colonise it, which then shapes the composition of subsequent colonists from the environment [9, 11, 22]. In either case, the host ensures a 'competitor-free space' for inherited microbes, which are allowed time and resources to grow on a new-born host before being exposed to competition with other colonists. For example, newly emerging *Acromyrmex* leafcutter ants are inoculated with antibiotic-producing *Pseudonocardia* bacteria within a 24-hour window after hatching [8, 25]. Mature worker ants serve as the source, carrying *Pseudonocardia* on their propleural plates,

which grow to high density around specialised exocrine glands that likely provide nutrients for bacterial growth [26, 27] (thus also serving as an example of a resource that can be metabolized by the preferred bacteria, discussed in 3. below). Similarly, female beewolf digger wasps (*Philanthus*, *Philanthinus*, *Trachypus*) inoculate their brood cell walls with species of *Streptomyces* that they maintain in their antennal glands [28, 29, 30]. These bacteria become directly incorporated into the larval cocoon, where they dominate and produce an array of antibiotics that protect the developing larva against infection [29, 30, 31]. Analogous to the above examples, the agricultural process of applying bacteria, such as antibiotic-producing *Pseudomonas* and nitrogen-fixing *Rhizobia*, to crop seeds before sowing mimics pseudo-vertical-transmission, by ensuring that high densities of beneficial bacteria have better access to root exudates and are favoured during establishment on the plant [32, 33]. Priority effects have also been demonstrated for mycorrhizae [34], bees [35, 36, 37, 38], wasps [28], leafcutter ants [25, 39], birds [40], plants [41], and humans [42].

2. *Hosts producing compounds poisoning non-desired bacteria, whilst allowing desired strains to grow*. — A wide range of plants secrete compounds, known as allelochemicals, that have toxic effects on a broad range of bacteria, fungi, and invertebrates in the rhizosphere, as well as other plants growing nearby [43, 44, 45, 46]. For example, the compound DIMBOA is an antimicrobial produced by maize seedlings [45], which the plant-beneficial species *Pseudomonas putida* is able to degrade, thus avoiding its effects. *P. putida* also uses this compound as a chemoattractant and a signal for upregulating the production of the broad-spectrum antibiotic phenazine [45]. Together, these mechanisms allow *P. putida* to colonise maize roots in the presence of mostly DIMBOA-intolerant, competitor bacteria [45]. Similarly, the rhizobial species, *Mesorhizobium tianshanense*, which forms root nodules on liquorice plants is able to outcompete other bacteria in the rhizosphere due to an efflux mechanism that confers resistance to the antimicrobial compound canavanine. Canavanine is abundant

in liquorice root exudates and thus allows the host to filter out non-beneficial rhizobial species [47].

As another example, nitric oxide (NO), a potent oxidising agent and antimicrobial, can play an important role in dictating symbiont specificity [48, 49]. A classic example arises during the symbiosis between the bobtail squid, *Euprymna scolopes*, and bioluminescent bacteria in the species *Vibrio fischeri*. *V. fischeri* are the exclusive colonisers of the squid's light organ, where they emit light to deceive predators, and are acquired horizontally from the environment within 48 hours after squid hatching [50]. High nitric-oxide synthase (NOS) activity and its product NO can be detected in the epithelial mucus of the light organ during the early stages of bacterial colonisation [51], which *V. fischeri* are able to tolerate via the activity of two proteins, flavohemoglobin (*Hmp*) and a heme NO/oxygen-binding protein (H-NOX) [52, 53, 54, 55]. Eliminating the genes for these proteins in *V. fischeri* leads to colonisation deficiency [53, 55], and diminishing the concentration of host NO results in a greater diversity of non-mutualistic bacterial species in the light organ epithelium [51]. Similar mechanisms of host selection are reported for animals as well. For example, members of the *Hydra* family produce antibacterial arminins that help them to shape the establishment of the bacterial microbiota during their embryogenesis [56]. *Hydra* not only suppress the undesired strains [56] but also modify the quorum-sensing signals through which bacteria communicate, hence manipulating the social behaviour of bacteria [57].

3. *A food resource that the desired partner is better able to metabolise*. — Enhanced metabolic activity from consuming a private resource can confer competitive superiority to a preferred microbial strain. Besides acquiring higher reproduction and growth rates, the beneficial bacteria can also achieve a higher rate of antibiotic production, resulting in the suppression of competitors [58], or a higher production of other factors that promote colonization and symbiotic interaction with the host, such as adhesive molecules facilitating biofilm formation on the host surface [59, 60]. The provision of specific metabolites is

thought to play a key role in structuring the species-specific microbial communities associated with marine corals [61, 62]. Coral juveniles, as well as their dinoflagellate symbionts, produce large quantities of the compound dimethylsulfoniopropionate (DMSP) [63]. *In vitro* and metagenomic studies have shown that several coral-associated bacterial groups can specifically metabolise the DMSP and use it as a sole carbon and sulphur source [61, 62, 64]. Such species are also amongst the first bacteria to colonise coral larvae, suggesting a nutritional advantage for them over bacteria that cannot degrade DMSP [61, 65]. This includes a species of *Pseudovibrio* which can additionally use DMSP as a precursor for the production of antibiotics which inhibit coral pathogens [62]. Another example of a specific host-derived resource is human breast milk, which is known to contain a large number of complex oligosaccharides that are preferentially consumed by a single species of co-adapted gut bacterium *Bifidobacterium longum* subsp. *infantis* [66].

In plants, experiments have shown that root exudates can be directly metabolised by the microorganisms that live endophytically within the plant roots [67, 68, 69]. Different species exude different groups of metabolites, and studies suggest that plant hosts may be able to tailor root exudate composition in order to recruit bacteria with particular metabolic traits [43, 67, 70]. For example, the concentration of the plant phytohormone salicylic acid (SA) has been shown to correlate with the abundance of several bacterial taxa, including the antibiotic-producing genus *Streptomyces* [70, 71], which can use SA as a sole carbon source [71, 72]. As discussed earlier, leaf-cutter ants exocrine glands which provide a nutrient source for *Pseudonocardia* bacterial growth also fall into this category [26].

These mechanisms achieve one of two effects: (i) they either ensure the protected growth of the preferred strains and/or (ii) they enhance the competitive abilities of preferred strains against non-preferred strains for certain duration of time. Essentially, a *host can use multiple means to provide a 'private resource', in the form of space and/or food, to a subset of bacterial strains*,

and if those strains are beneficial to the hosts, the host is selected to evolve and apply one or more of these mechanisms to assemble host-beneficial microbiomes.

We now abstract these mechanisms into an individual-based, spatially-explicit model of host-associated defensive microbiomes (reviews in 9, 29, 30), which typically contain antibiotic-producing, and at the same time resistant, bacteria [73, 74]. In our model, dispersal and *direct competition for empty sites* is limited to small numbers of neighbouring individuals, in accordance with experimental results [75]. At the same time, due to diffusion, we allow *indirect, antibiotic-mediated competition* to occur amongst distant bacteria. We aim to understand the conditions under which host species can promote the growth and dominance of antibiotic-producing, defensive microbiomes.

Materials and methods

We are interested in how the host influences the population dynamics of two different bacterial strains: an antibiotic-producing, resistant beneficial strain (**B**), and a non-producing, sensitive parasitic strain (**P**) (Fig. 1a). We model the host implicitly by assuming it is able to manipulate the composition of its microbiome through resource supply on its surface, upon which colonising individual bacteria compete for space with their neighbours according to their reproduction rates. The host surface further serves as a medium for spatially limited diffusion of the antibiotic. For this, we employ an individual-based model in which we model the host surface as a rectangular grid with toroidal boundary conditions ($N = M * M$) serving as the habitat for coloniser bacteria (Fig. 1b). Each grid point can be empty or inhabited by a single individual, and interactions take place within the immediate neighbourhood of the focal grid point. Time is measured in units of update steps. We assume that the dynamics of cell reproduction and death processes are much slower than the small-molecule dynamics, so the cell populations are updated after u ($u \gg 1$) update steps in antibiotic dynamics, during which the whole grid is updated in all relevant intracellular and extracellular processes related to the

small-molecule (antibiotic) dynamics (N number of sites). In the cellular update steps, εN number of randomly chosen grid cells are updated in the birth and death processes, and ε is selected to be a small positive number (see Supplementary information 1).

The private resource(s) provided by the host can confer two kinds of benefits to the beneficial strain. We call the first kind **Protected Growth** (recall mechanisms 1 and 2 from *Introduction)*, because *the parasitic strain is prevented from invading (i.e. colonising) the host until time* τ. Accordingly, **B** is given preferred access to host-provided food or space or is solely resistant to host-produced allelochemicals until time τ, after which time the host resource is made 'public' by giving the parasitic strain access to host-provided food or space or by withdrawing the host-produced compounds facilitating **B** or poisoning **P**. We call the second kind **Enhanced Metabolism**, because *although* **P** *is allowed to invade starting from time* 0*,* ***B****'s metabolism is enhanced until time* τ*, after which this enhancement lapses* (recall mechanism 3 from *Introduction*). The simplest outcome of enhanced metabolism is that **B**'s advantage in metabolising host-provided food causes its population growth rate to be increased by an amount of $r_{\mathrm{B,pr}}(t)$ until time τ, after which $r_{\mathrm{B,pr}}(t) = 0$ (e.g. $r_{\mathrm{B,pr}}(t) \geq 0 | t < \tau$ and $r_{\mathrm{B,pr}}(t) = 0 | t \geq \tau$), where index pr denotes the private resource. An alternative outcome is that **B** is able to use the host-provided food to *increase its own antibiotic production rate* ($\rho_{\mathrm{B}}(t) = \rho_{\mathrm{B,pr}}(t) + \rho_{\mathrm{B},0}$), without incurring higher unit costs. Thus, similarly as above, we distinguish a higher production rate fuelled by host-provided resource ($\rho_{\mathrm{B,pr}}(t) \geq 0 | t < \tau$), and a lower, baseline production rate when the resource is not supplied after time τ ($\rho_{\mathrm{B,pr}}(t) = 0 | t \geq \tau$). Naturally, $\rho_{\mathrm{B},0} > 0$, while the production rate of the non-producing strain is always zero ($\rho_{\mathrm{P}}(t) = 0$). (Alternatively, but not modelled here, the resource could allow the antibiotic to be effective at a lower threshold concentration before τ and at higher level after τ, which would give similar results to the previous).

Dynamics of the antibiotic molecules

The beneficial strain produces and exports antibiotic at rate ρ_{B}, into the extracellular environment, resulting in a distribution of concentrations $A^{\mathrm{Ext}}(i,t)$ at position i at time t.

The molecules are taken up by the cells at rates α_{B} and α_{P} ($\alpha_{\mathrm{B}} \leq \alpha_{\mathrm{P}}$) by the **B** and the **P** strains, respectively, resulting in an $A^{\mathrm{Int}}(i,t)$ interior concentration within the cell at position i at time t. The cells decompose the intracellular antibiotics at rates γ_{B} and γ_{P} ($\gamma_{\mathrm{B}} \geq \gamma_{\mathrm{P}}$), and they can also perform active outbound transport, i.e. controlled efflux, to release intracellular antibiotics at rates β_{B} and β_{P} ($\beta_{\mathrm{B}} \geq \beta_{\mathrm{P}}$). The antibiotics decays at rate φ in the environment.

The model implements the three major antibiotic-resistance mechanisms: (a) reduced influx through the membrane (α_{B}), (b) a higher rate of intracellular decomposition and neutralisation (γ_{B}), and (c) increased efflux of the molecules (β_{B}), and combinations of these mechanisms [73, 76, 77, 78, 79].

Based on the continuous reaction-diffusion model of the detailed dynamics (see Supplementary information 2 for details) [80], the time-and-space-discretised dynamics of antibiotic concentration at site i on the grid and at time $t + \Delta t$ in the extracellular environment can be written as

$$A^{\mathrm{Ext}}(i,t+\Delta t) = A^{\mathrm{Ext}}(i,t) + \left[\frac{D}{\Delta x^2}\left(\sum_{j=1}^{v} A^{\mathrm{Ext}}(j,t) - vA^{\mathrm{Ext}}(i,t)\right) + \left(\rho_*(t) + \beta_* A^{\mathrm{Int}}(i,t) - \alpha_* A^{\mathrm{Ext}}(i,t) - \varphi A^{\mathrm{Ext}}(i,t)\right)\theta(i)\right]\Delta t \quad (1)$$

where the first term corresponds to the diffusion of antibiotics according to the discretised diffusion algorithm between the four nearest neighbouring points ($v = 4$) (Neumann-neighbourhood: north, south, east, west); Δx is the spatial resolution, and Δt is the time resolution. The diffusion rate of the antibiotics, D, is measured in the unit of x^2/t, where x denotes the spatial resolution, here one cell of the grid, and t stands for time measured as an

update step. $\theta(\mathrm{i})$ takes the value one if there is a cell at the site i, else being zero. The dynamics of intracellular concentration of the antibiotic at the site i can be written as

$$A^{\mathrm{Int}}(i,t+\Delta t) = A^{\mathrm{Int}}(i,t) + \left(\alpha_* A^{\mathrm{Ext}}(i,t) - \beta_* A^{\mathrm{Int}}(i,t) - \gamma_* A^{\mathrm{Int}}(i,t)\right)\Delta t. \quad (2)$$

Naturally $A^{\mathrm{Int}}(i,t+\Delta t) = A^{\mathrm{Int}}(i,t) = A^{Ext}(i,t) = 0$ if there is no cell at site i.

Growth dynamics of the cells

For the birth and death processes, we define the growth rate of the antibiotic-producing (**B**) and non-producing (**P**) strains respectively as

$$r_{\mathrm{B}}(i,t) = r_{\mathrm{B},0} + r_{\mathrm{B,pr}}(t) - c, \quad (3)$$

$$r_{\mathrm{P}}(i,t) = r_{\mathrm{P},0} - \lambda(a,T,k,A^{\mathrm{Int}}(i,t))$$

where c is the decrease in reproduction rate because of the costly processes of antibiotic production and resistance. The reproduction rates $r_{\mathrm{B},0}$, $r_{\mathrm{P},0}$, and $r_{\mathrm{B,pr}}(t)$ correspond to normal (baseline) and temporarily increased resource conditions, respectively. The effect of the antibiotic $\lambda(a,T,k,A^{\mathrm{Int}}(i,t))$ on the **P** strain's reproduction rate depends on the critical threshold (T), the maximum effect (a), the steepness of the dosage effect (k), and the actual intracellular concentration of the antibiotic in the sensitive cell at the site i ($A^{\mathrm{Int}}(i,t)$). Following empirical observations [58], we define a general sigmoid function for the effect of the antibiotic:

$$\lambda\left(a,T,k,A^{\mathrm{Int}}(i,t)\right) = a/[1+\exp(-\mathrm{k}(A^{\mathrm{Int}}(i,t)-\mathrm{T}))] \quad (4)$$

Dynamics of the population

Population dynamics are represented by a death-birth process in which a randomly chosen focal individual at site i dies, and individuals from its Moore neighbourhood (8 nearest neighbours, $w = 8$) can reproduce and place a progeny into this focal empty site, with probability proportional to their growth rates

$$p(i) = r_\xi(i,t)/\textstyle\sum_{j=1}^{w} r_\xi(j,t), \text{ where } (\xi\epsilon\{\mathrm{P},\mathrm{B}\}) \quad (5)$$

At the beginning of the simulation, the beneficial strain is represented in low numbers ($n_{\mathrm{B},0}$), and the parasitic strain is missing ($n_{\mathrm{P},0} = 0$).

Invasion tests

We carried out two sets of invasion tests to demonstrate how host-provided private resources can result in self-sustaining, beneficial microbiomes, even if the advantage provided by the resource eventually diminishes. In the first test, we used time, while in the second, we used colony size as the signal to switch from private to public resources, or in other words, to stop the host's selective support for the beneficial strain.

Invasion test 1. Time-limited supply of private resources. — We model the two kinds of benefits conveyed by the private resources, as discussed earlier, the (1) Protected Growth of the beneficial strain for τ time and (2) the Enhanced Metabolism of the beneficial strain for τ time, either leading to (2a) a higher population growth rate by the beneficial strain or to (2b) an increased antibiotic production by the beneficial strain.

In the Protected Growth scenario, before τ, an s_+ proportion of cohesive space on the host surface ($s_+ = ss/N * 100$, where ss is the number of protected sites) provides a safe growth opportunity for the beneficial strain, as individuals from the parasitic strain are prevented from invading (strict and pseudo-vertical transmission), or parasitic individuals invading this region get killed off (via host-provided allelochemicals). Only after τ time has passed is the parasitic strain allowed to gain a foothold anywhere on the grid (empty or occupied). In other words, the private space resource becomes public at time τ. During an invasion attempt, we place $n_{\mathrm{P,t}} = 0$ number of individuals around a randomly selected focal grid point in a connected cluster with probability f in each time step (if there are empty places, subsequent individuals will be placed next to the focal site, but non-empty grid points can also be occupied if no empty places are available). In the Enhanced Metabolism scenario, the beneficial strain experiences increasing advantages of $r_+ = \left(r_{\mathrm{B,pr}}(t) + r_{\mathrm{B},0}\right)/r_{\mathrm{B},0} * 100$ or $\rho_+ = \left(\rho_{\mathrm{B,pr}}(t) + \rho_{\mathrm{B},0}\right)/\rho_{\mathrm{B},0} * 100$ for τ time,

respectively, and $n_{\mathrm{P,t}} = 0$ number of parasitic-strain individuals are allowed to invade with probability f in each time step, starting from the beginning.

Invasion test 2. Protected Growth of the beneficial strain to a minimum colony size. — Here, we let the host resource, the habitat, be private until the beneficial strain reaches a minimum colony size, which we call the Colony Size at Invasion (*CSI*). We only allow the parasitic strain to start invading empty places after the resident **B** strain's colony size has grown to the *CSI* ($CSI = q/N * 100$, where q is the number of sites inhabited by **B**). The invasion proceeds with probability f and with $n_{\mathrm{P,t}}$ number of invaders until the grid is fully occupied by individuals. As a motivating example, one can think of a small host 'crypt' in which beneficial strain is initially be housed, but the strain eventually outgrows the crypt and colonises the host surface, at which point, the host can only provide resources in a way that makes them publicly available.

Results

Invasion test 1. Time-limited supply of private resources. – As discussed in the *Introduction*, the host has multiple mechanisms by which it can provide private resources. We find that protecting initial growth (Fig. 2a, b), increasing the population growth rate (Fig. 2c, d), and/or enhancing the antibiotic effectiveness (Fig. 2e, f) of the beneficial strain can all result in a self-sustaining, beneficial-strain-dominated microbiome that is resistant to invasion even after the host resource is made public (at time τ) and the beneficial strain starts to experience a competitive disadvantage due to the costs of antibiotic production and of expressing its antibiotic-resistance traits. In all three scenarios, the longer the time τ that the resource is private (Fig. 2, x-axis), the less of an advantage, in the form of protected growth (here τ correlates with the size of the colony, see Supplementary information 1 Fig. 1), increased population growth (r_+), or increased antibiotic production (ρ_+) (y-axis), is required for the beneficial strain to be able to resist invasion after the resource becomes public. This is because

invasion resistance is dependent on the beneficial colony reaching a sufficiently large size and on the concentration of antibiotic the colony produces and transports into the environment.

We also observe that if the physiological mechanism of resistance by the beneficial strain to its own antibiotic is efflux, this can additionally enhance invasion resistance, even if the supply time is short and the advantage conferred by the private resource is small (Fig. 2a, b, c vs. e, d, f). The reason is that re-exporting any ingested antibiotic increases the environmental concentration of antibiotic, which aids suppression of invading parasitic strains.

Invasion test 2. Protected Growth of the beneficial strain until a minimum colony size. – Consistent with the results from Invasion test 1, if the beneficial colony reaches a critical size, (the Minimum Sustainable Colony size: *MSC*) it becomes resistant to invasion over a wide range of parameters after the private resource is made public (Fig. 3). Again, having antibiotic efflux as the resistance mechanism promotes invasion resistance (Fig. 3 and 4), whereas (and intuitively) a higher rate of extracellular decay of antibiotic counteracts this effect (Fig. 3 and 4). When a large amount of antibiotic is in the environment, because efflux is high and decay is low (Fig. 3a and Fig. 4a, c), the beneficial strain is able to dominate over a wide range of diffusion rates. However, when efflux is weak and the extracellular decay rate is high, only high diffusion rates allow the beneficial strain to dominate (Fig. 4d). This is because at low diffusion rates, the antibiotic produced in the centre of the colony is lost due to decomposition before reaching the colony edge by diffusion, where it would have attacked invaders. In contrast, at high diffusion rates, more of the resident colony's antibiotic production is recruited to fight invasion (Fig. 3, 4, and 5).

The complement to this result is that if the diffusion rate is low, then even a large colony size does not necessarily guarantee success unless the efflux rate is also high enough (Fig. 4a, b). Essentially, if antibiotic efflux is used as the resistance mechanism by the beneficial cells, this can substitute for outright diffusion of the antibiotic, allowing the antibiotic to reach the colony edge, where it can suppress invaders (Fig. 4).

Non-monotonous effect of diffusion. — Interestingly, under some conditions there is a non-monotonous effect of diffusion rate on invasion resistance, such that the Minimum Colony Size (*MSC*) can be much smaller for medium-level diffusion rates. For example, looking at Fig. 3b, for low antibiotic diffusion rates (values $0-1$ on the x-axis), the *MSC* is close to 100%; that is, the colony can resist invasion only if more than 95% of the available habitat is already occupied by the producers; otherwise, parasites displace the whole population of antibiotic producers. Similarly, for high diffusion rates (values $D = 80-100$ on the x-axis), although smaller, but a considerable colony size still has to be reached. However, the *MSC* curve reaches a minimum between low and high diffusion rates, such that only a $1-10\%$ *MSC* is enough to resist invasion (Fig. 3b).

The important result is that for any intermediate efflux and decay parameters and with intermediate diffusion rates, *colonies with practically any non-zero initial size can withstand parasite invasion* (Fig. 3a, b, d). This nonlinearity occurs because, in general, diffusion carries antibiotic to the edge of the antibiotic-producing colony, where it can act against invading **P** strains, but diffusion also carries antibiotic *away from* the edge of the colony. An intermediate diffusion rate turns out to maximise the amount of antibiotic at the fighting front.

Discussion

The composition of host-associated microbiomes has been shown to correlate with host health status and fitness [4, 81, 82, 83, 84, 85, 86, 87], and thus, there is likely strong selection on host species to evolve mechanisms that favour the assembly of certain kinds of microbiomes over others [11, 12, 27]. Here we have explored how a host can favour the assembly of a defensive microbiome dominated by antibiotic-producing bacteria, hence promoting colonization resistance, in a competitive set-up [7, 23, 74, 88].

We argue that a host can take advantage of an ecological phenomenon known as *bistability*. When two species compete via interference, such as when a bacterial species uses antibiotics

to hinder a competitor, the winner of the competition depends partially on the initial population sizes of the two species [9]. If the antibiotic-producer establishes itself with a larger population in the new habitat, it can collectively produce sufficient amount of antibiotic to suppress its competitor and grow until the space of opportunity vanishes for the parasite. In contrast, if the non-producer species starts with the larger or competitively superior population, then the small amount of antibiotic produced by the small colony of the producer is insufficient to suppress the non-producer, hence it wins.

It follows that by using an antibiotic-producer as the initial (or 'priming') strain of the microbiome, a host can narrow down the variety of strains able to invade this already established environment [4, 5, 9, 11]. The host is thus efficiently able to canalise the composition of the emerging microbiome. Such priming effects have been demonstrated in various experimental systems [25, 37, 39, 89].

We integrated local interactions and explicit spatial dynamics of cellular and chemical components in our model with the original phenomenological model that laid the foundations if the theory [9]. In this more realistic model, even for large populations, the number of directly interacting cells is relatively modest, and spatial correlations of active agents determine dynamics meaningfully [5, 75]. Furthermore, such an integrated, spatially-explicit model allows us to understand the effect of different antibiotic-resistance mechanisms [73, 76, 77, 78, 79, 80, 90] on the microbiome assembly, and to investigate how attributes of the host surface, which govern the diffusion dynamic of the antibiotic, can modify the outcome. We have also widened the applicability of Scheuring and Yu's model [9] by reviewing multiple mechanisms allowing a host to prime a defensive microbiome, even if the beneficial can only be recruited from the environment (horizontal transmission), compared to the original model, which made the restrictive assumption that the beneficial strain is strictly vertically transmitted.

We have corroborated the earlier results [9, 13] that antibiotic producers and non-producers can form a bistable system and that the outcome of competition depends on their reproduction

rates, how effectively the host is able to selectively promote the beneficial strain, and the initial ratio of the two strains [9]. Once the antibiotic producer is able to gain dominance, in such a system, it can remain dominant for a lifetime, even if the host-provided private resource vanishes or becomes public. The current model also shows that localized interactions do not impede this dominance because the antibiotic itself can diffuse, eventually reaching the colony edge to inhibit invaders. This effect is strengthened when the mode of resistance by the producers is antibiotic efflux.

We also show with the current model that the host resource only needs to remain private for a finite critical time, basically until the beneficial colony reaches a Minimal Sustainable Colony Size (*MSC*), at which point it becomes resistant to a given rate of invasion. The critical time and/or the *MSC* depends on the physiochemical properties of the system, most importantly the decomposition, decay, diffusion, and efflux rates of the antibiotic, and the advantage provided to the beneficial colony by the private resource, all deriving from the fact that colony size determines the amount of antibiotic produced.

Our brief review of the literature suggests that multiple forms of ‘private resources’ exist, including food, space, or host-provided compounds harming undesired strains. Nonetheless, privacy of resources is inherently difficult and costly to achieve, and it is therefore realistic to assume that any host-provided resources will eventually become public. This inevitable transition from private to public, which intuitively might be expected to allow the successful invasion and establishment of parasitic strains, *does not in fact do so*, because of bistability. After a beneficial colony establishes itself, a public resource is in practice only enjoyed by the winner, the beneficial colony.

Finally, we show that an intermediate diffusion rate can maximise the amount of antibiotic accumulating at the colony edge. Our findings suggest that the attributes of the host surface, for example the diffusion rate, can either increase or reduce the effect range of the antibiotic [91]. As there is no conflict of interest between antibiotic-producer and host, their coevolution is

expected to optimize the diffusion speed, and hence the effectiveness, of the antibiotic. Overall, evolutionary optimisation can act by minimising the host investment required to attain a beneficial microbiome, by reducing the duration of a private resource supply, and by evolving the optimal physiochemical properties of the habitat, the host surface. If so, then we might also expect that the co-evolution of host and preferred strains results in an efficient and well-conducted build-up of a beneficial microbiome, an orchestrated symbiosis that efficiently narrows down the enormous number of possible scenarios to canalise the emergence of the microbiome towards the most favourable one.

Acknowledgements

We acknowledge KIFÜ for awarding us access to resource based in Hungary at Budapest, Debrecen, and Szeged. We acknowledge supports from OTKA grants Nr. K100299, and GINOP grant Nr. 2.3.2-15-2016-00057. S.F.W. was funded by a NERC PhD studentship (NERC Doctoral Training Progamme grant NE/L002582/1). D. W. Yu was supported by the National Natural Science Foundation of China (41661144002, 31670536, 31400470, 31500305), the Key Research Program of Frontier Sciences, CAS (QYZDY-SSW-SMC024), the Bureau of International Cooperation project (GJHZ1754), the Ministry of Science and Technology of China (2012FY110800), the University of East Anglia, the State Key Laboratory of Genetic Resources and Evolution at the Kunming Institute of Zoology, and the University of Chinese Academy of Sciences.

Conflicts of interest

The authors declare no conflict of interest.

References

1. Costello EK, Stagaman K, Dethlefsen L, Bohannan BJM, Relman DA. The application of ecological theory toward an understanding of the human microbiome. *Science* 2012; 336: 1255–1262.
2. Levy R, Borenstein E. Metabolic modeling of species interaction in the human microbiome elucidates community-level assembly rules. *Proc Natl Acad Sci U S A* 2013; 110: 12804–12809.
3. Weber MF, Poxleitner G, Hebisch E, Frey E, Opitz M. Chemical warfare and survival strategies in bacterial range expansions. *J R Soc Interface* 2014; 11: 20140172.
4. McNally L, Brown SP. Building the microbiome in health and disease: niche construction and social conflict in bacteria. *Phil Trans R Soc Lond B Biol Sci* 2015; 370: 20140298.
5. Cordero OX, Datta MS. Microbial interactions and community assembly at microscales. *Curr Opin Microbiol* 2016; 31: 227–234.
6. Li L, Ma Z. Testing the neutral theory of biodiversity with human microbiome datasets. *Sci Rep* 2016; 6: 31448.
7. García-Bayona L, Comstock LE. Bacterial antagonism in host-associated microbial communities. *Science* 2018; 361: pii: eaat2456.
8. Zhang MM, Poulsen M, Currie CA. Symbiont recognition of mutualistic bacteria by *Acromyrmex* leaf-cutting ants. *ISME J* 2007; 1: 313–320.
9. Scheuring I, Yu DW. How to assemble a beneficial microbiome in three easy steps. *Ecol Lett* 2012; 15: 1300–1307.
10. Coyte KZ, Schluter J, Foster KR. The ecology of the microbiome: Networks, competition, and stability. *Science* 2015; 350: 663–666.
11. Foster KR, Schluter J, Coyte KZ, Rakoff-Nahoum S. The evolution of the host microbiome as an ecosystem on a leash. *Nature* 2017; 548: 43–51.

12. Duarte A, Welch M, Swannack C, Wagner J, Kilner RM. Strategies for managing rival bacterial communities: Lessons from burying beetles. *J Anim Ecol* 2018; 87: 414–427.
13. Innocent T, Holmes N, Al Bassam M, Schiott M, Scheuring I, Wilkinson B et al. Experimental demonstration that screening can enable the environmental recruitment of a defensive microbiome. *bioRxiv* 2018; https://doi.org/10.1101/375634.
14. Green JL, Bohannan BJ, Whitaker RJ. Microbial biogeography: from taxonomy to traits. *Science* 2008; 320: 1039–1043.
15. Jeraldo P, Sipos M, Chia N, Brulc JM, Dhillon AS, Konkel ME et al. Quantification of the relative roles of niche and neutral processes in structuring gastrointestinal microbiomes. *Proc Natl Acad Sci U S A* 2012; 109: 9692–9698.
16. Fondi M, Karkman A, Tamminen MV, Bosi E, Virta M, Fani R et al. “Every gene is everywhere but the environment selects”: Global geolocalization of gene sharing in environmental samples through network analysis. *Genome Biol Evol* 2016; 8: 1388–1400.
17. Engl T, Kroiss J, Kai M, Nechitaylo TY, Svatoš A, Kaltenpoth M. Evolutionary stability of antibiotic protection in a defensive symbiosis. *Proc Natl Acad Sci U S A* 2018; 115: E2020–E2029.
18. West SA, Diggle SP, Buckling A, Gardner A, Griffin AS. The social lives of microbes. *Annu Rev Ecol Evol Syst* 2007; 38: 53–77.
19. Bull JJ, Rice WR. Distinguishing mechanisms for the evolution of co-operation. *J Theor Biol* 1991; 149: 63–74.
20. Herre EA, Knowlton N, Mueller UG, Rehner SA. The evolution of mutualisms: exploring the paths between conflict and cooperation. *Trends Ecol Evol* 1999; 14: 49–53.
21. Sachs JL, Mueller UG, Wilcox TP, Bull JJ. The evolution of cooperation. *Q Rev Biol* 2004; 79: 135–160.
22. Ebert D. The epidemiology and evolution of symbionts with mixed-mode transmission. *Ann Rev Ecol Evol Syst* 2013; 44: 623–643.

23. Clay K. Defensive symbiosis: a microbial perspective. *Funct Ecol* 2014; 228: 293–298.
24. Frank S. Host-symbiont conflict over the mixing of symbiotic lineages. *Proc R Soc Lond B Biol Sci* 1996; 263: 339–344.
25. Marsh SE, Poulsen M, Pinto-Tomás A, Currie CR. Interaction between workers during a short time window is required for bacterial symbiont transmission in *Acromyrmex* leaf-cutting ants. *PLoS ONE* 2014; 9: e103269.
26. Currie CR, Poulsen M, Mendenhall J, Boomsma JJ, Billen J. Coevolved crypts and exocrine glands support mutualistic bacteria in fungus-growing ants. *Science* 2006; 311: 81–83.
27. Li H, Sosa-Calvo J, Horn HA, Pupo MT, Clardy J, Rabeling C et al. Convergent evolution of complex structures for ant–bacterial defensive symbiosis in fungus-farming ants. *Proc Natl Acad Sci U S A* 2018; e-pub ahead of print 3 October 2018; doi:10.1073/pnas.1809332115.
28. Kaltenpoth M, Göttler W, Herzner G, Strohm E. Symbiotic bacteria protect wasp larvae from fungal infestation. *Curr Biol* 2005; 15: 475–479.
29. Kaltenpoth M. *Actinobacteria* as mutualists: general healthcare for insects? *Trends Microbiol* 2009; 17: 529–535.
30. Seipke RF, Kaltenpoth M, Hutchings MI. *Streptomyces* as symbionts: an emerging and widespread theme? *FEMS Microbiol Rev* 2012; 36: 862–876.
31. Kroiss J, Kaltenpoth M, Schneider B, Schwinger MG, Hertweck C, Maddula RK et al. Symbiotic *Streptomycetes* provide antibiotic combination prophylaxis for wasp offspring. *Nat Chem Biol* 2010; 6: 261–263.
32. O'Callaghan M. Microbial inoculation of seed for improved crop performance: issues and opportunities. *Appl Microbiol Biotechnol* 2016; 100: 5729–5746.
33. Deaker R, Roughley RJ, Kennedy IR. Legume seed inoculation technology – a review. *Soil Biol Biochem* 2004; 36: 1275–1288.
34. Werner GDA, Kiers ET. Order of arrival structures arbuscular mycorrhizal colonization of plants. *New Phytol* 2014; 205: 1515–1524.

485 35. Vojvodic S, Rehan SM, Anderson KE. Microbial gut diversity of Africanized and European
486 honey bee larval instars. *PLoS ONE* 2013; 8:e72106.
487 36. Powell JE, Martinson VG, Urban-Mead K, Moran NA. Routes of acquisition of the gut
488 microbiota of *Apis mellifera*. *Appl Environ Microbiol* 2014; 80: 7378–7387.
489 37. Schwarz RS, Moran NA, Evans JD. Early gut colonizers shape parasite susceptibility and
490 microbiota composition in honey bee workers. *Proc Natl Acad Sci U S A* 2016; 113: 9345–
491 9350.
492 38. Kwong WK, Moran NA. Gut microbial communities of social bees. *Nat Rev Microbiol* 2016;
493 14: 374–384.
494 39. Andersen SB, Yek SH, Nash DR, Boomsma JJ. Interaction specificity between leaf-cutting
495 ants and vertically transmitted *Pseudonocardia* bacteria. *BMC Evol Biol* 2015; 15: 27.
496 40. Martínez-García Á, Martín-Vivaldi M, Rodríguez-Ruano SM, Peralta-Sánchez JM, Valdivia
497 E, Soler JJ. Nest bacterial environment affects microbiome of hoopoe eggshells, but not
498 that of the uropygial secretion. *PLoS ONE* 2016; 11: e0158158.
499 41. Truyens S, Weyens N, Cuypers A, Vangronsveld J. Changes in the population of seed
500 bacteria of transgenerationally Cd-exposed *Arabidopsis thaliana*. *Plant Biol* 2012; 15: 971–
501 981.
502 42. Turnbaugh PJ, Hamady M, Yatsunenko T, Cantarel BL, Duncan A, Ley RE et al. A core gut
503 microbiome in obese and lean twins. *Nature* 2009; 457: 480–484.
504 43. Bais HP, Weir TL, Perry LG, Gilroy S, Vivanco JM. The role of root exudates in rhizosphere
505 interactions with plants and other organisms. *Annu Rev Plant Biol* 2006; 57: 233–66.
506 44. Hartmann A, Schmid M, van Tuinen D, Berg G. Plant-driven selection of microbes. *Plant*
507 *Soil* 2008; 321: 235–257.
508 45. Neal AL, Ahmad S, Gordon-Weeks R, Ton J. Benzoxazinoids in root exudates of maize
509 attract *Pseudomonas putida* to the rhizosphere. *PLoS ONE* 2012; 7: e35498.

510 46. De Coninck B, Timmermans P, Vos C, Cammue BP, Kazan K. What lies beneath:
511 belowground defense strategies in plants. *Trends Plant Sci* 2015; 20: 91–101.
512 47. Cai T, Cai W, Zhang J, Zheng H, Tsou AM, Xiao L et al. Host legume-exuded
513 antimetabolites optimize the symbiotic rhizosphere. *Mol Microbiol* 2009; 73: 507–517.
514 48. Fang FC. Antimicrobial reactive oxygen and nitrogen species: concepts and controversies.
515 *Nat Rev Microbiol* 2004; 2: 820–832.
516 49. Wang Y, Ruby EG. The roles of NO in microbial symbioses. *Cell Microbiol* 2011; 13: 518–
517 526.
518 50. Mandel MJ, Dunn AK. Impact and influence of the natural vibrio-squid symbiosis in
519 understanding bacterial-animal interactions. *Front Microbiol* 2016; 15: 1982.
520 51. Davidson SK, Koropatnick TA, Kossmehl R, Sycuro L, McFall-Ngai MJ. NO means 'yes' in
521 the squid-vibrio symbiosis: nitric oxide (NO) during the initial stages of a beneficial
522 association. *Cell Microbiol* 2004; 6: 1139–1151.
523 52. Ruby EG, McFall-Ngai MJ. Oxygen-utilizing reactions and symbiotic colonization of the
524 squid light organ by *Vibrio fischeri*. *Trends Microbiol* 1999; 7: 414–420.
525 53. Poole RK, & Hughes MN. New functions for the ancient globin family: bacterial responses
526 to nitric oxide and nitrosative stress. *Mol Microbiol* 2000; 36: 775–783.
527 54. Wang Y, Dufour YS, Carlson HK, Donohue TJ, Marletta MA, Ruby EG. H-NOX-mediated
528 nitric oxide sensing modulates symbiotic colonization by *Vibrio fischeri*. *Proc Natl Acad Sci*
529 *U S A* 2010; 107: 8375–8380.
530 55. Wang Y, Dunn AK, Wilneff J, McFall-Ngai MJ, Spiro S, Ruby EG. *Vibrio fischeri*
531 flavohaemoglobin protects against nitric oxide during initiation of the squid–*Vibrio*
532 symbiosis. *Mol Microbiol* 2010; 78: 903–915.
533 56. Franzenburg S, Walter J, Künzel S, Wang J, Baines JF, Bosch TCG et al. Distinct
534 antimicrobial peptide expression determines host species-specific bacterial associations.
535 *Proc Natl Acad Sci U S A* 2013; 110: E3730–E3738.

57. Pietschke C, Treitz C, Forêt S, Schultze A, Künzel S, Tholey A et al. Host modification of a bacterial quorum-sensing signal induces a phenotypic switch in bacterial symbionts. *Proc Natl Acad Sci U S A* 2017; 114: E8488–E8497.
58. Bernier SP, Surette MG. Concentration-dependent activity of antibiotics in natural environments. *Front Microbiol* 2013; 13: 20.
59. Schluter J, Nadell CD, Bassler BL, Foster KR. Adhesion as a weapon in microbial competition. *ISME J* 2015; 9: 139–149.
60. McLoughlin K, Schluter J, Rakoff-Nahoum S, Smith AL, Foster KR. Host selection of microbiota via differential adhesion. *Cell Host Microbe* 2016; 19: 550–559.
61. Raina J-B, Dinsdale EA, Willis BL, Bourne DG. Do the organic sulfur compounds DMSP and DMS drive coral microbial associations. *Trends Microbiol* 2010; 18: 101–108.
62. Raina J-B, Tapiolas D, Motti CA, Foret S, Seemann T, Tebben J et al. Isolation of an antimicrobial compound produced by bacteria associated with reef-building corals. *PeerJ* 2016; 18: e2275.
63. Raina J-B, Tapiolas DM, Foret S, Lutz A, Abrego D, Ceh J et al. DMSP biosynthesis by an animal and its role in coral thermal stress response. *Nature* 2013; 502: 677–680.
64. Raina J-B, Tapiolas DM, Willis BL, Bourne DG. Coral-associated bacteria and their role in the biogeochemical cycling of sulfur. *Appl Environ Microbiol* 2009; 75: 3492–3501.
65. Apprill A, Marlow HQ, Martindale MQ, Rappé MS. The onset of microbial associations in the coral *Pocillopora meandrina*. *ISME J* 2009; 3: 685–699.
66. Zivkovic AM, German JB, Lebrilla CB, Mills DA. Human milk glycobiome and its impact on the infant gastrointestinal microbiota. *Proc Natl Acad Sci U S A* 2011; 108: 4653–4658.
67. Haichar FZ, Marol C, Berge O, Rangel-Castro JI, Prosser JI, Balesdent J et al. Plant host habitat and root exudates shape soil bacterial community structure. *ISME J* 2008; 2: 1221–1230.

561 68. Badri DV, Vivanco JM. Regulation and function of root exudates. *Plant Cell Environ* 2009;
562 32: 666–681.
563 69. Dennis PG, Miller AJ, Hirsch PR. Are root exudates more important than other sources of
564 rhizodeposits in structuring rhizosphere bacterial communities? *FEMS Microbiol Ecol* 2010;
565 72: 313–327.
566 70. Badri DV, Chaparro JM, Zhang R, Shen Q, Vivanco JM. Application of natural blends of
567 phytochemicals derived from the root exudates of *Arabidopsis* to the soil reveal that
568 phenolic-related compounds predominantly modulate the soil microbiome. *J Biol Chem*
569 2013; 288: 4502–4512.
570 71. Lebeis SL, Paredes SH, Lundberg DS, Breakfield N, Gehring J, McDonald M et al. Salicylic
571 acid modulates colonization of the root microbiome by specific bacterial taxa. *Science* 2015;
572 349: 860–864.
573 72. Ishiyama D, Vujaklija D, Davies J. Novel pathway of salicylate degradation by *Streptomyces*
574 *sp*. strain WA46. *Appl Environ Microbiol* 2004; 70: 1297–1306.
575 73. Wright GD. Mechanisms of resistance to antibiotics. *Curr Opin Chem Biol* 2003; 7: 563–
576 569.
577 74. Ghoul M, Mitri S. The ecology and evolution of microbial competition. *Trends Microbiol*
578 2016; 24: 833–845.
579 75. Raynaud X, Nunan N. Spatial ecology of bacteria at the microscale in soil. *PLoS ONE*
580 2014; 9: e87217.
581 76. Wright GD. Bacterial resistance to antibiotics: enzymatic degradation and modification. *Adv*
582 *Drug Deliv Rev* 2005; 57: 1451–1470.
583 77. Kumar A, Schweizer HP. Bacterial resistance to antibiotics: active efflux and reduced
584 uptake. *Adv Drug Deliv Rev* 2005; 57: 1486–513.
585 78. Marquez B. Bacterial efflux systems and efflux pumps inhibitors. *Biochimie* 2005; 87: 1137–
586 1147.

587 79. Davies J, Davies D. Origins and evolution of antibiotic resistance. *Microbiol Mol Biol Rev*
588 2010; 74: 417–433.
589 80. Kondrat S, Zimmermann O, Wiechert W, von Lieres E. Discrete-continuous reaction-
590 diffusion model with mobile point-like sources and sinks. *Eur Phys J E* 2016; 39: 11.
591 81. Rodriguez R, Redman R. More than 400 million years of evolution and some plants still
592 can't make it on their own: plant stress tolerance via fungal symbiosis. *J Exp Bot* 2008; 59:
593 1109–1114.
594 82. Lau JA, Lennon JT. Evolutionary ecology of plant–microbe interactions: soil microbial
595 structure alters selection on plant traits. *New Phytol* 2011; 192: 215–224.
596 83. Rolli E, Marasco R, Vigani G, Ettoumi B, Mapelli F, Deangelis ML et al. Improved plant
597 resistance to drought is promoted by the root-associated microbiome as a water stress-
598 dependent trait. *Environ Microbiol* 2014; 17: 316–31.
599 84. Wang ZK, Yang YS, Stefka AT, Sun G, Peng LH. Review article: fungal microbiota and
600 digestive diseases. *Aliment Pharmacol Ther* 2014; 39: 751–766.
601 85. Mueller UG, Sachs JL. Engineering microbiomes to improve plant and animal health.
602 *Trends Ecol Evol* 2015; 23: 606–617.
603 86. Shreiner AB, Kao JY, Young VB. The gut microbiome in health and in disease. *Curr Opin*
604 *Gastroenterol* 2015; 31: 69–75.
605 87. Lloyd-Price J, Abu-Ali G, Huttenhower C. The healthy human microbiome. *Genome Med*
606 2016; 8: 51.
607 88. Lloyd DP, Allen RJ. Competition for space during bacterial colonization of a surface. *J R*
608 *Soc Interface* 2015; 12: 20150608.
609 89. Haichar FZ, Santaella C, Heulin T, Achouak W. Root exudates mediated interactions
610 belowground. *Soil Biol Biochem* 2014; 77: 69–80.
611 90. Wright GD. Antibiotic resistance in the environment: a link to the clinic? *Curr Opin Microbiol*
612 2010; 13: 589–594.

613 91. Harcombe WR, Riehl WJ, Dukovski I, Granger BR, Betts A, Lang AH et al. Metabolic
614 resource allocation in individual microbes determines ecosystem interactions and spatial
615 dynamics. *Cell Metab* 2014; 7: 1104–1115.

Figures

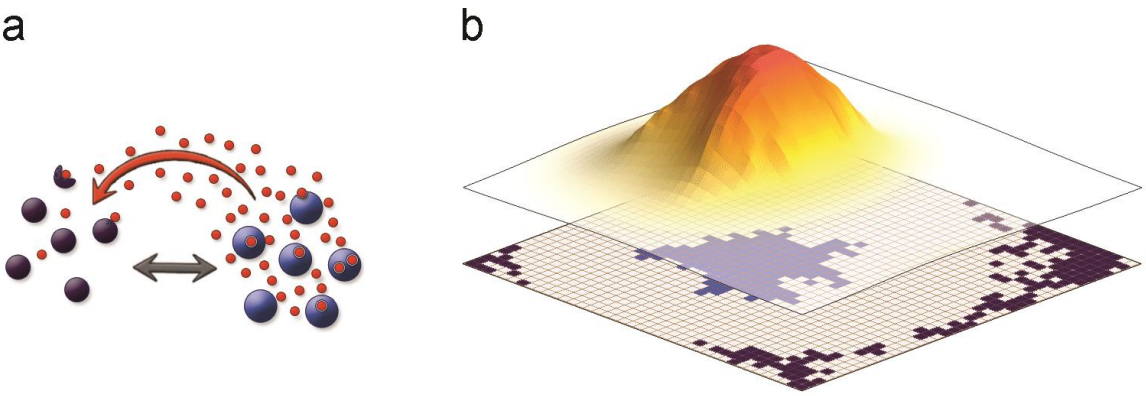

Figure 1. **a** We model two types of strains, parasitic (violet shading) and antibiotic-producer (blue shading), which compete with each other directly (grey arrow), and indirectly via the diffusing antibiotic (red dots and coloured arrows). **b** The modelled $N = M * M$ grid (bottom layer) represents the colonisable surface of the host, and each point in the grid can be inhabited by a single individual (coloured quadrant). The produced antibiotic (upper layer) diffuses freely on the grid, and its concentration decreases farther from the producing source (the shading and height depicting the concentration) and also decays with time. Relevant model parameters are: $D = 5,\ \Delta t = 1/10,\ u = 100,$ for **a** $n_{\mathrm{B},0} = 100,\ N = 10\,000,$ and for **b** $n_{\mathrm{B},0} = 1,\ M = 40,\ \rho = 1,$ $\alpha_{\mathrm{B}} = 0.5, \beta_{\mathrm{B}} = 0.6, \gamma_{\mathrm{B}} = 0.3, \varphi = 0.5.$

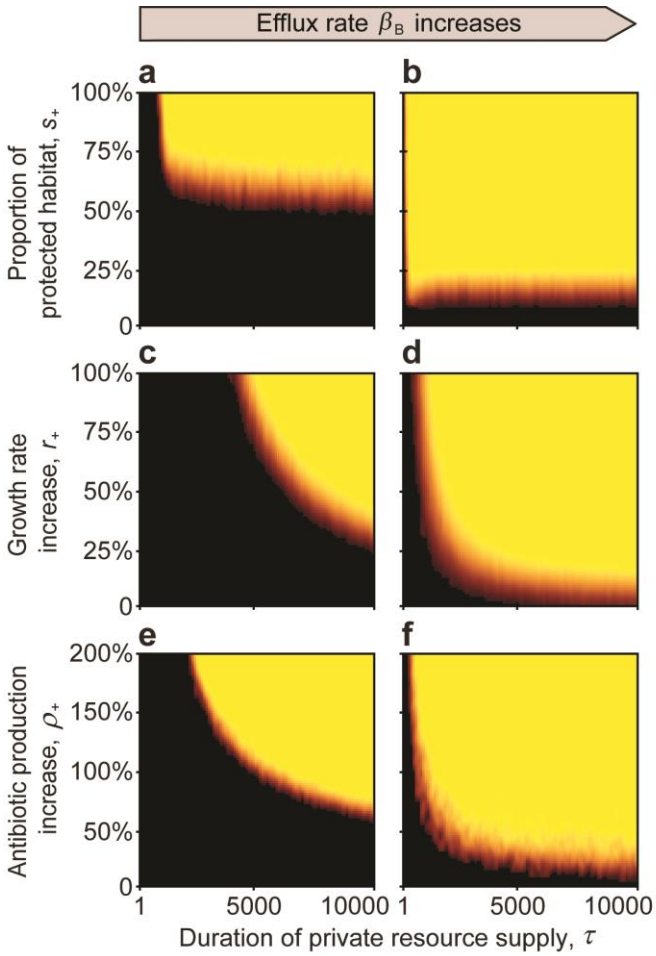

627

628 **Figure 2.** The effect of a private resource supplied by the host for a limited time τ (*Invasion Test*
629 *1*). Black areas indicate parameter space where the non-producing parasitic strain can invade,
630 and yellow indicates that the beneficial strain is able to resist invasion. Orange to red colours
631 indicate mixed outcomes. In general, the beneficial strain (yellow) dominates over a larger
632 proportion of the parameter space as the duration of the private resource supply lengthens,
633 regardless of whether the beneficial strain enjoys outright protected growth (**a**, **b**), an increased
634 rate of population growth (**c**, **d**), or an increased rate of antibiotic production (**e**, **f**). The efflux of
635 accumulated intracellular antibiotic in the antibiotic-producing beneficial strain also aids
636 beneficial-strain dominance ($\beta_B = 0$ for **a**, **c**, **e**, and $\beta_B = 0.25$ for **b**, **d**, **f**). Simulations were run
637 with 5 replicates for $100\,000$ generations or until the population was homogenous. Model
638 parameters are: $r_{B,0} = 0.8,\ r_{P,0} = 0.8,\ c = 0.1,\ \rho_{B,0} = 1,\ \alpha_B = 0.5,\ \alpha_P = 0.5,\ \beta_P = 0,\ \gamma_B = 0.4,$
639 $\gamma_P = 0.4,\ D = 5,\ a = 1,\ T = 1,\ k = 25,\ N = 10\,000,\ n_{B,0} = 100,\ n_{P,t} = 10,\ f = 0.01,\ D = 5,$
640 $\Delta t = 1/10,\ u = 100,\ \varphi = 0.3$ for **a**, **b**, **c**, **d**, $\varphi = 0.4$ for **e**, **f**, and $r_{B,pr}(t) = 0$, and $\rho_{B,pr}(t) = 0$
641 when applicable.

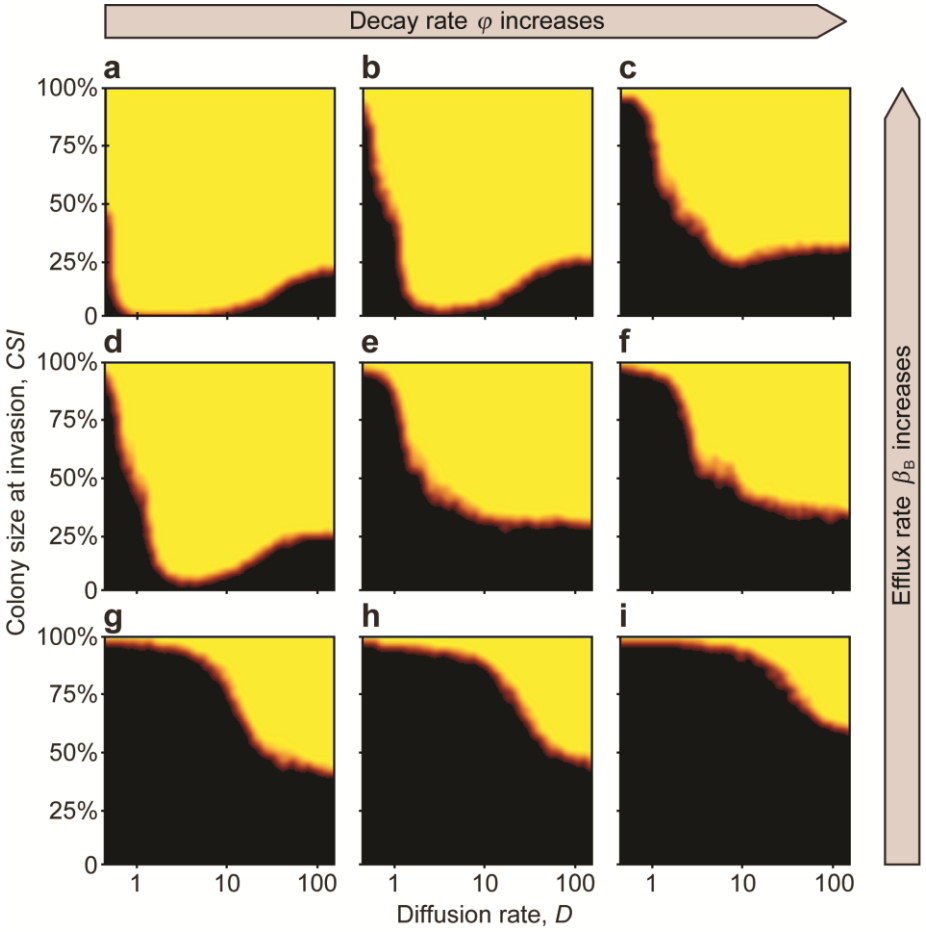

Figure 3. The Minimal Sustainable Colony size (*MSC*) (*Invasion Test 2*). Invasion is initiated when the beneficial-strain colony reaches a defined size (*CSI*) and continues until the habitat is fully colonized by either the beneficial or the parasitic strains. The *MSC* is represented by the orange-red border separating the yellow (**B** wins) and black (**P** wins) regions. From left to right (**a**→**c**, **d**→**f**, and **g**→**i**), the φ extracellular decay rate of the antibiotic increases ($\varphi = 0.2, 0.25, 0.3$). From top to bottom (**a**→**g**, **b**→**h**, and **c**→**i**), the efflux rate β_B decreases ($\beta_B = 1, 0.5, 0$). Simulations were run with 3 replicates for $100\,000$ generations, or until the population was homogenous. Black areas indicate parameter space where the parasitic strain can invade, yellow indicates parameter space where the antibiotic-producing beneficial strain successfully resists invasion, and orange areas correspond to mixed outcomes. Model parameters are: : $r_{B,0} = 0.8,\ r_{P,0} = 0.8,\ r_+ = 0,\ c = 0.4,\ \rho_{B,0} = 1,\ \rho_+ = 0,\ \alpha_B = 0.5,\ \alpha_P = 0.5,\ \beta_P = 0,\ \gamma_B = 0.4,\ \gamma_P = 0.4,\ D = 5,\ a = 1,\ T = 1,\ k = 25,\ N = 10\,000,\ n_{B,0} = 100,\ n_{P,t} = 10,\ f = 0.01,\ \Delta t = 1/10,\ u = 100.$

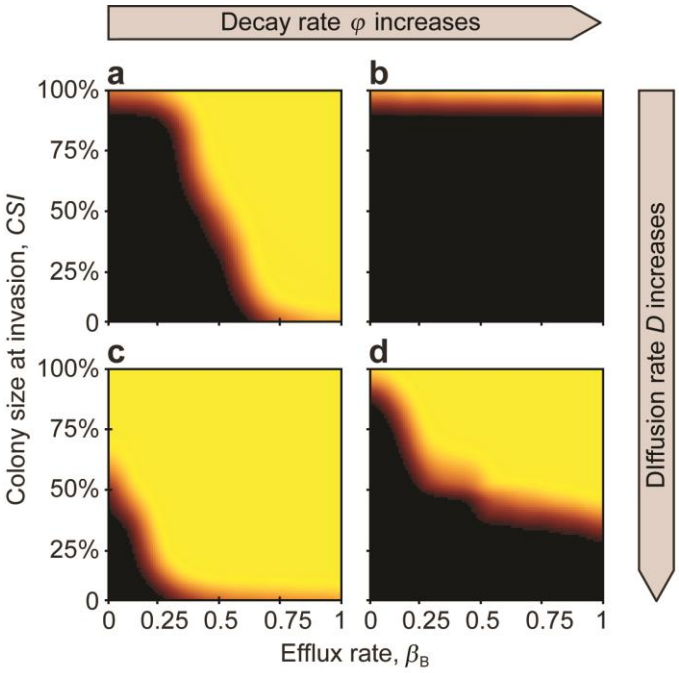

Figure 4. The effect of efflux rate, decay rate, and diffusion rate on the *MSC*. At low diffusion rates (upper row), efflux rate limits the success, while at large diffusion rate (bottom row), colony size is the more limiting factor. From left to right (**a**→**b**, **c**→**d**) extracellular decay rate increases ($\varphi = 0.7$ and 0.9). From the top to the bottom (**a**→**c**, and **b**→**d**), diffusion rate increases ($D = 0.5$ and 12), respectively. Model parameters are: $r_{\mathrm{B},0} = 0.8$, $r_{\mathrm{P},0} = 0.8$, $r_{+} = 0$, $c = 0.1$, $\rho_{\mathrm{B},0} = 1$, $\rho_{+} = 0$, $\alpha_{\mathrm{B}} = 0.6$, $\alpha_{\mathrm{P}} = 0.6$, $\beta_{\mathrm{P}} = 0$, $\gamma_{\mathrm{B}} = 0.3$, $\gamma_{\mathrm{P}} = 0.3$, $a = 1$, $T = 1$, $k = 25$, $\tau = 300$, $N = 10\,000$, $n_{\mathrm{B},0} = 100$, $n_{\mathrm{P,t}} = 10$, $f = 0.01$, $\Delta t = 1/10$, $u = 100$.

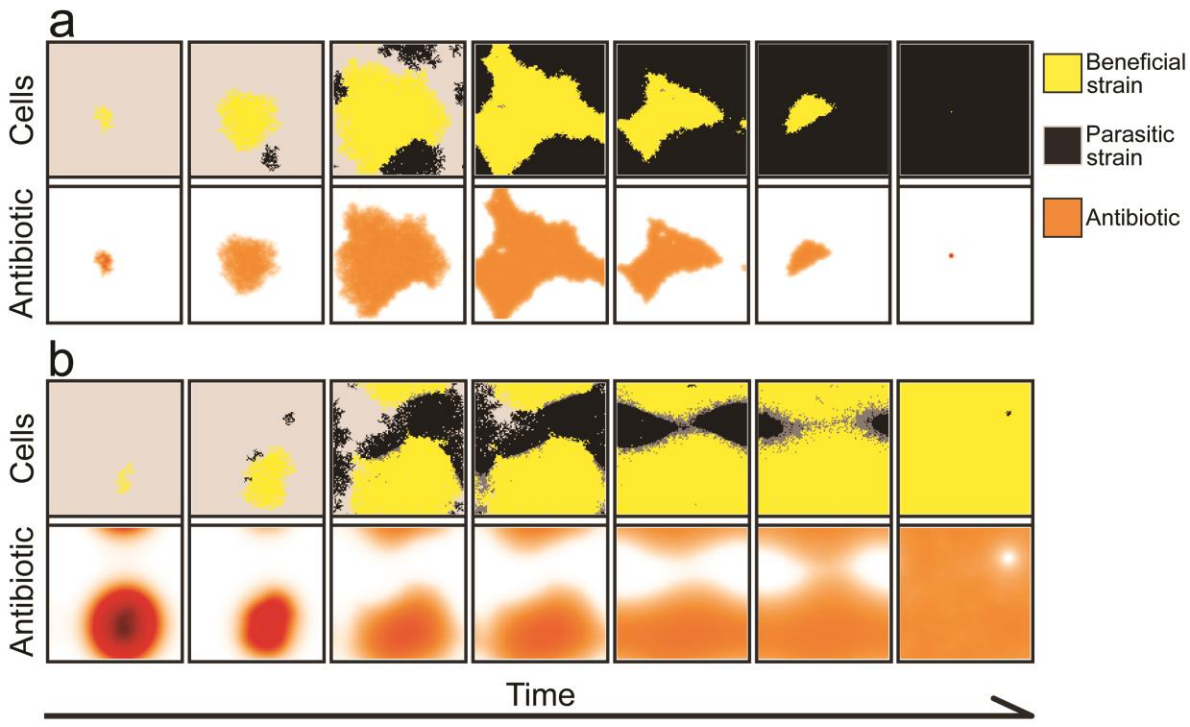

Figure 5. The spatial dynamics for **(a)** low ($D = 0.5$) and **(b)** high diffusion ($D = 50$) rates. **a** A low diffusion rate reduces the protective effect of the antibiotic (orange shading, lower panels), and the parasitic strain (black shading, upper panels) can invade the beneficial strain (yellow shading, upper panels). **b** A high diffusion rate allows the beneficial strain to resist invasion, as considerable amount of antibiotic (lower panels) diffuses beyond the colony boundaries. Antibiotic concentration ranges between zero (white), to intermediate (red-orange), to maximal concentrations (brown-black). Poisoned (cells with $r_{\mathrm{P}} < 0.05$) but not yet removed parasitic cells are coloured grey. In these simulations, the beneficial colony was allowed $\tau = 300$ time steps to grow before invasion. The snapshots of the simulations are taken every 30 update steps. Model parameters are: $r_{\mathrm{B},0} = 0.8$, $r_{\mathrm{P},0} = 0.8$, $r_{+} = 0$, $c = 0.4$, $\rho_{\mathrm{B},0} = 1$, $\rho_{+} = 0$, $\alpha_{\mathrm{B}} = 0.5$, $\alpha_{\mathrm{P}} = 0.5$, $\beta_{\mathrm{B}} = 0.4$, $\beta_{\mathrm{P}} = 0$, $\gamma_{\mathrm{B}} = 0.4$, $\gamma_{\mathrm{P}} = 0.4$, $\varphi = 0.25$, $a = 1$, $T = 1$, $k = 25$, $\tau = 300$, $N = 10\,000$, $n_{\mathrm{B},0} = 100$, $n_{\mathrm{P,t}} = 10$, $f = 0.01$, $\Delta t = 1/10$, $u = 100$.

Supplementary information

Supplementary information 1. The growth dynamic of a colony in the individual-based model. The colony growth follows a logistic growth dynamic in the model (Supplementary Fig. 1). Depending on the choice of ε, we observe full colonisation of the surface within a given timeframe. To better investigate the competition dynamics between the two types on a fine timescale, we choose $\varepsilon = 0.01$ for our investigations.

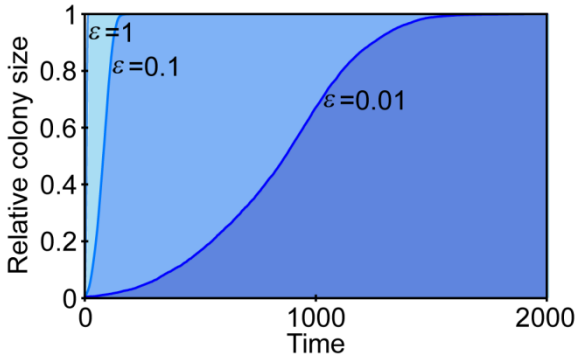

Supplementary Figure 1.

The growth dynamic of a colony follows a logistic trend in the model. We show the relative colony size (y-axis) with respect to time (x-axis) with $\varepsilon = 1$ (light blue), $\varepsilon = 0.1$ (medium blue), and $\varepsilon = 0.01$ (dark blue), where ε is the fraction of randomly chosen grid cells that is updated in the cellular reproduction and death processes. The smaller the ε, the slower the growth in our model. Relevant model parameters are: $\mathrm{D} = 5$, $\Delta t = 1/10$, $u = 100$, for **a** $n_{\mathrm{B},0} = 100, N = 10\,000$.

Supplementary information 2. Mathematical formulation of the reaction-diffusion dynamics for the mean-field model.

We assume that the antibiotic molecules are point-like particles moving on a host-surface plane. Consequently, we can use reaction-diffusion dynamics to describe change in the extracellular antibiotic concentration $A^{Ext}(\mathbf{x},t)$ at points $\mathbf{x}=(x,y)$ (representing the coordinates on a surface) and times *t*

(6)

$$\frac{\partial A^{Ext}(\mathbf{x},t)}{\partial t} = D\left(\frac{\partial^2 A^{Ext}(\mathbf{x},t)}{\partial x^2} + \frac{\partial^2 A^{Ext}(\mathbf{x},t)}{\partial y^2}\right) + F\left(A^{Ext}(\mathbf{x},t)\right)$$

where the first term on the right hand side is the diffusion term, and $F\left(A^{Ext}(\mathbf{x},t)\right)$ is the reaction term, which depends on the extracellular antibiotic concentration (A^{Ext}) and the positions and types of the cells. Using the above defined parameters and dynamical processes, we can write

(7)

$$F\left(A^{\mathrm{Ext}}(\mathbf{x},t)\right) = \sum_{i=1}^{N}\left(\rho_*(t) + \beta_* A^{\mathrm{Int}}(i,t) - \alpha_* A^{\mathrm{Ext}}(i,t)\right)\delta(\mathbf{x}-i) - \varphi A^{\mathrm{Ext}}(i,t),$$

where the antibiotic sources and sinks are summed in the parentheses, i is the position of a cell among the N cells, which can either be **B** or **P** denoted by $*$ in the bottom index where applicable, $A^{\mathrm{Int}}(i,t)$ is the intracellular concentration of the antibiotic at position i, and δ is the Dirac delta [80].